Supplemental Document

Optical Materials EXPRESS

Comparison and analysis of phase change materials-based reconfigurable silicon photonic directional couplers: supplement

Ting Yu Teo,[1,4] Milos Krbal,[2] Jan Mistrik,[2,3] Jan Prikryl,[2] Li Lu,[1] and Robert Edward Simpson[1,5]

[1] *Singapore University of Technology and Design, 8 Somapah Road, 487372 Singapore, Singapore*
[2] *University of Pardubice, Faculty of Chemical Technology, Center of Nanomaterials and Nanotechnologies (CEMNAT), Legions Square 565, 530 02 Pardubice, Czech Republic*
[3] *University of Pardubice, Faculty of Chemical Technology, Institute of Applied Physics and Mathematics, Studentska 95, 532 10 Pardubice, Czech Republic*
[4] *tingyu_teo@mymail.sutd.edu.sg*
[5] *robert_simpson@sutd.edu.sg*

Supplement DOI: https://doi.org/10.6084/m9.figshare.17372090

Parent Article DOI: https://doi.org/10.1364/OME.447289

A comparison and analysis of phase change materials-based reconfigurable silicon photonic directional couplers: supplemental document

1. Material Fabrication

This section describes the material fabrication process of Sb_2S_3 and Sb_2Se_3 used in the ellipsometry measurements.

1.1 Sb_2Se_3

The Sb_2Se_3 material was prepared from a bulk sample with $Sb_{36}Se_{64}$ composition by direct synthesis from 5N elements. A total of 30 g of elements was placed in a quartz ampoule, evacuated to 10^{-3} Pa and then sealed. The ampoule was then placed in a rocking furnace and exposed to 950°C for 24h at a heating rate of 1°C/min and finally quenched in cold water.

Amorphous Sb_2Se_3 thin films with the thickness of 200 nm were then deposited by pulsed laser deposition in the off-axis geometry using a KrF laser with the wavelength of 248 nm, the pulse length of 30 nm. The laser frequency was 5Hz, with an output intensity of 2.1 J/cm^2. A distance between the $Sb_{36}Se_{64}$ target and a substrate holder was about 5 cm. The deposition was performed under a residual pressure $7x10^{-5}$Pa (a residual pressure after deposition $6x10^{-5}$ Pa) at room temperature. A silicon wafer and fused silica were used as substrates. Prior to opening the chamber, the deposited samples remained under vacuum for an additional 2 hours to cool down and release tension. After film deposition, we performed EDX (Energy Dispersive X-Ray Analysis) on the samples. The mean Sb: Se atomic percentage is 39.9 : 60.1.

Half of the amorphous Sb_2Se_3 samples were crystallized in a tube furnace at 250 °C for 2h under an inert argon atmosphere to prevent oxidation of the samples by air. X-ray diffraction reflectivity (XRD) measurements were conducted to ensure that the films are fully crystallized. Amorphous and crystalline states of Sb_2Se_3 were probed by X-ray diffraction using a diffractometer (Empyrean Malvern Panalytical) operated in 2theta/omega mode to fully satisfy the Bragg-Brentano geometry. The XRD scans in Fig S1 shows the readings before and after crystallization. The XRD crystalline peaks obtained in Fig S1 were consistent with the data obtained from the National Institute for Material Science, Japan (NIMS) crystal database [1].

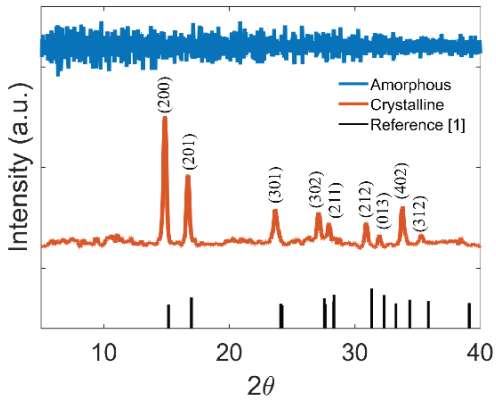

Fig. S1: XRD measurements of the Sb_2Se_3 films before and after crystallization.

1.2 Sb_2S_3

Sb_2S_3 thin films were deposited by Radio Frequency magnetron sputtering using the AJA Orion 5 sputtering system with a base pressure of 3.9×10^{-7} Torr. The Sb_2S_3 material come from a commercially purchased target with diameter of 50.8 mm and purity of 99.9%. The sputtering process took place in an Argon environment at a pressure of 3.7×10^{-3} Torr. The RF power was set to 40 W, which resulted in a deposition rate of 0.93 Å/s. After film deposition, we performed EDX (Energy Dispersive X-Ray Analysis) on the samples. The mean Sb: S atomic percentage is 37.4 : 62.6.

To determine the phase transition temperature, we measured the change in reflectivity of a Sb_2S_3 thin film during the annealing process. These measurements were done before preparing the actual samples for ellipsometry measurements. The sample was from the same sputtering batch as the ones we used in the ellipsometry measurements to ensure consistency. The phase transition of the material is represented by an abrupt change in reflectivity [2]. Fig. S2a shows the change of reflectivity with increasing temperature. The sample was crystallized on a Linkam heating stage (Linkam T95-HT) at a heating rate of 5 ℃/s to 320 ℃. To prevent oxidation, Ar gas of 4 SCCM was supplied to the heating enclosure. We then fit a sigmoid function to the trend shown in Fig. S2a. The equation was then differentiated to determine the phase transition temperature. Note, the equation does not bear any physical meaning and was used to simplify the differentiation operation. Fig. S2b shows the differentiated curve, with the maximum peak to be at 300 ℃. This corresponds to the phase transition temperature. Upon determining the phase transition to be 300 ℃ we crystallized the Sb_2S_3 thin film at 320 ℃ with a heating ramp rate of 5 ℃/s and hold time of 10 minutes to be used for ellipsometry measurements. Note that the phase transition temperature here is higher than the value reported for Sb_2S_3 strips in fig. 8c. This is because under the same measured area (same optical microscope magnification), a larger volume of material is being crystallized for the thin film sample. For the same heating ramp rate of 5℃/min, we reach a higher temperature before the larger volume of material is fully crystallized.

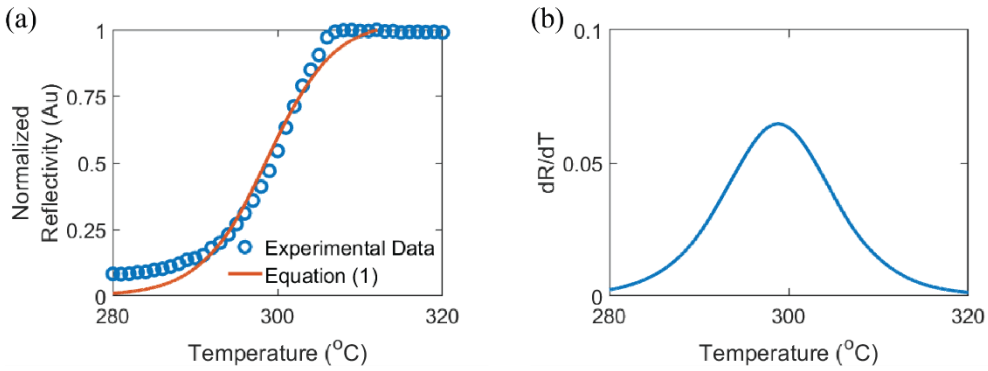

Fig. S2: Reflectivity measurements of Sb_2S_3 thin films to determine the phase transition temperature. (a) Change in reflectivity with respect to the change in temperature. (b) Differential of (a). A sigmoid function was fitted into (a) to simplify the differential operation.

2. Ellipsometry Measurements

Spectra of ellipsometric parameters were recorded by VASE ellipsometer (J.A. Woollam, Co.). For Sb_2Se_3, the incidence angles were 60° to 80°, covering the spectral range from 190 to 1800 nm, whilst for Sb_2S_3 the incidence angles were 50°, 60°, and 70°, covering the spectral range from 250 to 2000 nm. Reflectance and transmittance measurements were carried out by the same instrument and were treated simultaneously along with ellipsometry by WVASE commercial software. The ellipsometric spectroscopy, as an indirect characterization, requires a design of a sample model including material optical constants (in the form of table data or parameterized dielectric functions). The sample model consisted of a substrate (naively oxidized crystalline Si or transparent fused quartz) covered by the material films. Slight surface roughness was accounted by Bruggeman effective medium approximation [3] with 50% of the voids.

Optical constants of crystalline Si and its native oxide were taken from the software database. Native oxide thickness and fused quartz refractive index were determined by preliminary ellipsometric measurements on blank substrates. For both materials, dielectric functions of the amorphous films were parameterized by a single Tauc-Lorenc oscillator, whereas the polycrystalline films were parameterized by a sum of Tauc-Lorentz and Lorentz oscillators.

3. Sb_2S_3 and Sb_2Se_3 Bandgap Derivation

The band gaps of both amorphous materials were obtained from the Tauc-Lorentz model used to fit our ellipsometry measurements. In the crystalline state, the band gap could not be directly obtained from the Tauc- Lorentz model as the additional oscillators contribute to the near infrared absorption. Hence the band gap of both materials were determined from a Tauc-plot. We report band gap of energies of 1.58 eV and 1.06 eV for Sb_2S_3 and Sb_2Se_3, respectively from the Tauc-plot shown in fig. S3.

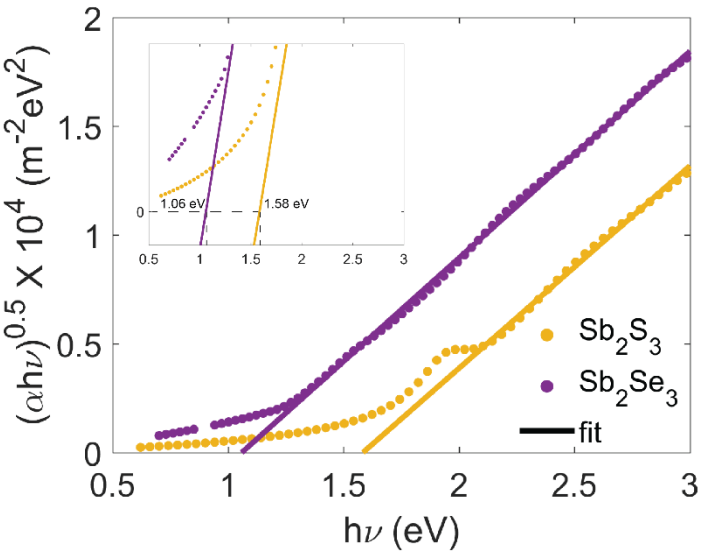

Fig. S3: Tauc plot of crystalline Sb_2S_3 and Sb_2Se_3

4. Field distribution profile of PCM directional couplers

The k values for each PCM material at the C Band used in our simulation models are shown in table S1.

Table S1. Optical Constants of the four PCM @ 1550 nm used in the simulation model

PCM	k value wavelength/wavelength range (μm)	
	Amorphous	Crystalline
$Ge_2Sb_2Te_5$	0.0365581 1.55	1.11305 1.55
$Ge_2Sb_2Se_4Te_1$	0.007623898 1.55	0.444633977 1.55
Sb_2Se_3	0 – 0 1.51 – 1.57	0.148207– 0.141335 1.51 – 1.57
Sb_2S_3	0 – 0 1.51 – 1.59	0.020483 – 0.0191 1.51 – 1.59

In our ellipsometry measurements for Sb_2S_3 and Sb_2Se_3, the k values are obtained from discrete wavelength measurements. Hence a range was provided instead. The simulation software interpolates the k values at 1550 nm.

Using the data from table S1, the effective refractive index of the PCM waveguides were calculated using Lumerical's MODE solution solver. The resulting value are shown in Table S2. This was to determine the width of the bar waveguides to attain phase matching condition in the amorphous state. The calculated odd and even supermodes in the two-waveguide system shown in Table S3 were used to determine the coupling length. Fig. S4. shows the corresponding E-field intensity distribution of the PCM waveguide in both isolated and two-waveguide system.

Table S2. Effective refractive index of the single PCM waveguides in Fig. S1.

	Amorphous	Crystalline
$Ge_2Sb_2Te_5$	$2.29 + 0.00228i$	$2.57 + 0.220i$
$Ge_2Sb_2Se_4Te_1$	$2.24 + 0.000314\,i$	$2.34 + 0.0375i$
Sb_2S_3	$2.22 + 6.77 \times 10^{-5}i$	$2.24 + 0.000790\,i$
Sb_2Se_3	$2.24 + 5.09 \times 10^{-8}i$	$2.30 + 0.00927i$

Table S3a. Odd and even supermodes of the two-waveguide system in Figs. S4(a) and S4(b).

		$Ge_2Sb_2Te_5$		$Ge_2Sb_2Se_4Te_1$	
		Amorphous	Crystalline	Amorphous	Crystalline
Even mode	n	2.32	2.57	2.25	2.34
	k	0.00110	0.217	0.000146	0.0370
Odd mode	n	2.27	2.30	2.23	2.24
	k	0.00114	0.000991	0.000167	0.000367

Table S3b. Odd and even supermodes of the two-waveguide system in Figs. S4(c) and S4(d).

		Sb_2S_3		Sb_2Se_3	
		Amorphous	Crystalline	Amorphous	Crystalline
Even mode	n	2.22	2.24	2.26	2.30
	k	9.22×10^{-8}	0.000735	6.61×10^{-8}	0.008551
Odd mode	n	2.21	2.22	2.23	2.24
	k	4.14×10^{-8}	5.31×10^{-5}	2.67×10^{-8}	0.000651

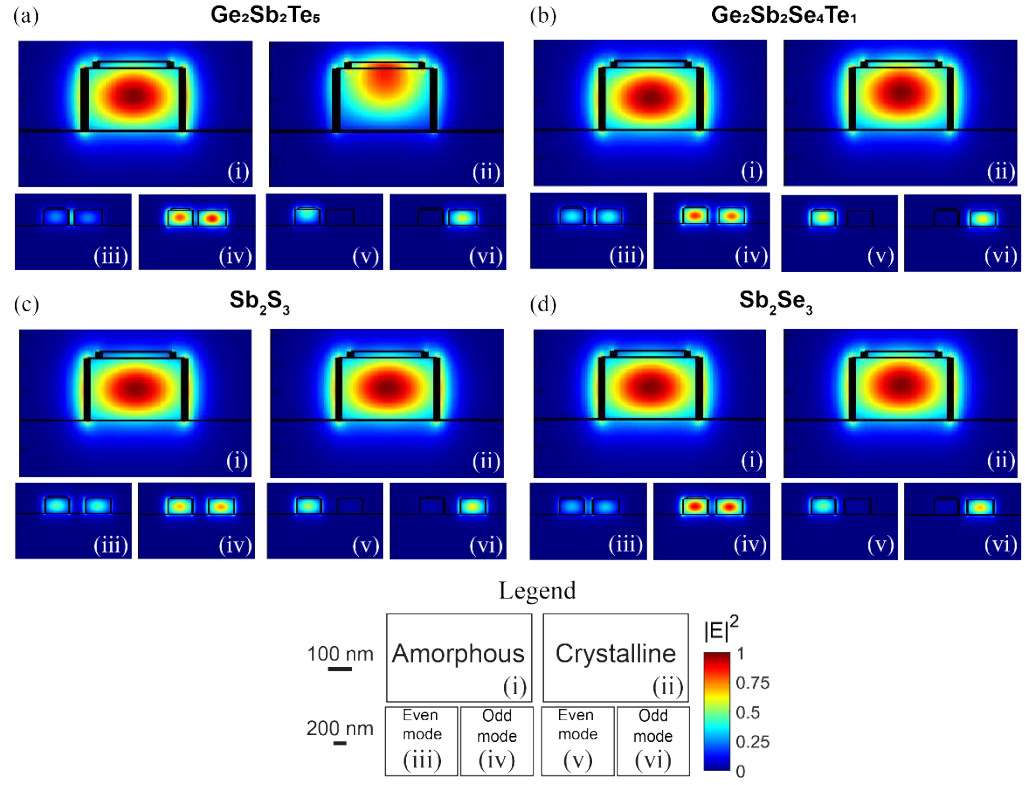

Fig. S4. Electric field intensity distribution of the following PCM -integrated waveguides: (a) GST, (b) GSST, (c) Sb_2S_3 and (d) Sb_2Se_3. (i) and (ii) show the electric field distribution of a single PCM-integrated waveguide in the amorphous and crystalline state respectively. (iii) and (v) show the corresponding even modes while (iv) and (vi) show the odd modes in the two-waveguide system. As the change in refractive index upon phase transition, Δn, increases, the mode pattern shown in (ii) is confined to the PCM material when it crystallizes. A small Δn cause the mode distribution to remain in the Si waveguide when the material crystallizes.

5. Sb_2S_3 strip

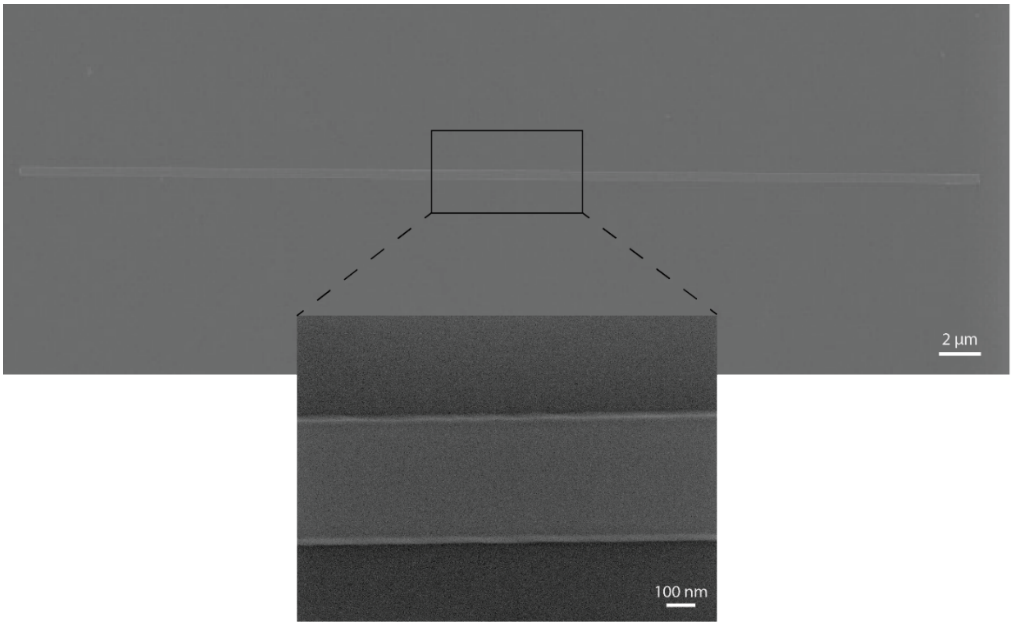

Fig. S5. SEM image of a typical Sb_2S_3 strip used in the partial crystallization experiment. Dimensions of the strip are similar to the optimized dimension in Table 1.

References

1. "National Institute of Material Science Crystal Database", retrieved 28 October 2021, https://crystdb.nims.go.jp/index.html.
2. N. Yamada, E. Ohno, K. Nishiuchi, N. Akahira, and M. Takao, "Rapid-phase transitions of GeTe-Sb2Te3 pseudobinary amorphous thin films for an optical disk memory," Journal of Applied Physics **69**, 2849-2856 (1991).
3. D. A. G. Bruggeman, "Berechnung verschiedener physikalischer Konstanten von heterogenen Substanzen. I. Dielektrizitätskonstanten und Leitfähigkeiten der Mischkörper aus isotropen Substanzen," Annalen der Physik **416**, 636-664 (1935).